THE FATE OF ACCRETING WHITE DWARFS: TYPE I SUPERNOVAE VS. COLLAPSE

BNL--38509

DE86 015949

Ken'ichi Nomoto

Department of Physics, Brookhaven National Laboratory
Upton, NY 11973, U.S.A.

on leave from the Department of Earth Science and Astronomy
College of Arts and Sciences, University of Tokyo
Meguro-ku, Tokyo 153, Japan

A lecture delivered at International School of Nuclear Physics, 10th Course
The Early Universe and Its Evolution
Erice, April 2 - 14, 1986

to be published in *Progress in Particle and Nuclear Physics*, Vol 18, 1986

THE FATE OF ACCRETING WHITE DWARFS: TYPE I SUPERNOVAE VS. COLLAPSE

Ken'ichi Nomoto

Department of Physics, Brookhaven National Laboratory
Upton, NY 11973, U.S.A.

on leave from the Department of Earth Science and Astronomy
College of Arts and Sciences, University of Tokyo
Meguro-ku, Tokyo 153, Japan

ABSTRACT

The final fate of accreting C+O white dwarfs is either thermonuclear explosion or collapse, if the white dwarf mass grows to the Chandrasekhar mass. We discuss how the fate depends on the initial mass, age, composition of the white dwarf and the mass accretion rate. Relatively fast accretion leads to a carbon deflagration at low central density that gives rise to a Type Ia supernova. Slower accretion induces a helium detonation that could be observed as a Type Ib supernova. If the initial mass of the C+O white dwarf is larger than 1.2 $M_{\odot}$, a carbon deflagration starts at high central density and induce a collapse of the white dwarf to form a neutron star. We examine the critical condition for which a carbon deflagration leads to collapse, not explosion. For the case of explosion, we discuss to what extent the nucleosynthesis models are consistent with spectra of Type Ia and Ib supernovae.

KEYWORDS

Accretion; white dwarfs; neutron star; X-ray star; nucleosynthesis: supernovae.

I. INTRODUCTION

The final fate of accreting white dwarfs has attracted a lot of recent attention because it is related to the origin of Type I supernovae and low mass X-ray binaries. In fact, the exploding white dwarf model, in particular, the carbon deflagration model is in good agreement with many of the observations of Type Ia supernovae (Nomoto 1986a; Woosley and Weaver 1986b). For Type Ib supernovae, currently most popular models are explosions of Wolf-Rayet stars. However, it has been suggested that the maximum light spectrum can better be explained by off-center explosions of white dwarfs. Recent observations of several interesting binary systems, low mass X-ray binaries, QPOs, and binary radio pulsars have suggested that in these systems a neutron star has formed from accretion-induced collapse of a white dwarf (van den Heuvel 1984; Taam and van den Heuvel 1986). Therefore, we have a good reason to believe that at least some accreting white dwarfs increase their mass to the Chandrasekhar mass, though the exact evolution of the binary systems leading to the supernova stage is not yet known.

These variations in the final fate of accreting white dwarfs originate from the difference in the parameters of the binary system, i.e., composition, mass, and age of the white dwarf, its companion star, and, in particular, mass accretion rate. We discuss first how these parameters determine the condition of nuclear burning in white dwarfs and then how the ignition condition determines the hydrodynamical outcome.

The case of explosion has been studied extensively in modeling Type Ia supernovae (Nomoto 1986a; Woosley and Weaver 1986b). On the other hand, the collapse of white dwarfs has been explored only for some specific condition and not for a wide range of parameter space. Therefore, we will discuss here the case of collapse in most detail in order to clarify the following point.

Possible models for the white dwarf collapse involve solid C+O white dwarfs, in which carbon and oxygen may or may not have chemically separated (Canal and Isern 1979; Isern et al. 1983) and O+Ne+Mg white dwarfs (Nomoto et al. 1979). For a wide range of mass accretion rates and initial white dwarf masses, the O+Ne+Mg white dwarfs collapse due to electron capture on ^{24}Mg and ^{20}Ne (Nomoto 1980; Miyaji et al. 1980). On the other hand, depending on the conditions of the white dwarfs and binary systems in which they are formed, the C+O white dwarfs could either explode or collapse. Chemical separation in such objects is still hypothetical and in any case could not be complete before carbon burning starts (Mochkovici 1983). It takes a carbon fraction of only a few percent to sustain a deflagration.

Therefore, it is worth determining the critical condition for which a carbon deflagration induces the collapse of a C+O white dwarf rather than its explosion. Such a condition has been obtained for the carbon detonation (Bruenn 1972; Mazurek et al. 1974) but not for the carbon deflagration except for certain specific models (Ivanova et al. 1974; Isern et al. 1985). We have performed numerical simulations of conductive and convective deflagrations starting from $\rho_c \sim 10^{10}$ g cm^{-3} and found that the C+O white dwarf collapses if the propagation velocity is slower than $\sim 0.15\ v_s$ (v_s is the sound speed). Generally, for both conductive and convective deflagrations, this is the case.

In the next section, the fate of accreting white dwarfs are summarized in the parameter space of accretion rate and the initial mass of the white dwarfs. In §3 and §4, models for Type Ia and Ib supernovae are presented focusing on the comparison between nucleosynthesis yield and the maximum light spectra. In §5, possibilities of white dwarf collapse is examined. Finally the fate of merging white dwarfs are discussed for the He - He white dwarf pair, and C+O - C+O pair.

II. EFFECTS OF ACCRETION AND THE FATE OF WHITE DWARFS

Isolated white dwarfs are simply cooling stars that eventually end up as *dark matter*. In binary systems they evolve differently because mass accretion from their companion provides gravitational energy that rejuvenates them. The gravitational energy released at the accretion shock near the stellar surface is radiated away and does not heat the white dwarf interior. However, the compression of the interior by the accreted matter releases additional gravitational energy. Some of this energy goes into thermal energy (compressional heating) and the rest is transported to the surface and radiated away (radiative cooling). Therefore, the interior temperature is determined by the balance between heating and cooling and, thus, strongly depends on the mass accretion rate, $\dot{M}$ (Nomoto 1982a, 1984b).

Compression first heats up a layer near the surface because of the small pressure scale height there. Later, heat diffuses inward as seen from the change in the temperature distribution in Figure 1. The diffusion timescale depends on $\dot{M}$ and is small for larger $\dot{M}$'s because of the large heat flux and steep temperature gradient generated by rapid accretion. For example, the time it takes the heat wave to reache the central region is about 2×10^5 yr for $\dot{M} \sim 10^{-6}\ M_\odot$ yr^{-1} (Figure 1) and 5×10^6 yr for $\dot{M} \sim 4 \times 10^{-8}\ M_\odot$ yr^{-1}. Therefore, if the initial mass of the white dwarf, M_{CO}, is smaller than 1.2 $M_\odot$, the entropy in the center has increased substantially due to the heat inflow when the white dwarf mass becomes 1.4 $M_\odot$. On the other hand, if the white dwarf is sufficiently massive and cold at the onset of accretion, the central region is compressed only adiabatically and thus is cold when carbon burning is ignited in the center. In the latter case, the ignition density is as high as 10^{10} g cm^{-3} (e.g., Isern et al. 1983).

Figure 2 shows how the density at the carbon ignition depends on the accretion rate. Shown is the evolutionary path of (ρ_c, T_c) at the center of accreting C+O white dwarfs for two cases. For $\dot{M} = 4 \times 10^{-8}\ M_\odot\ \mathrm{yr}^{-1}$, carbon deflagration is ignited at relatively low density ($\rho_c \simeq 3 \times 10^9\ \mathrm{g\ cm}^{-3}$). This model is in good agreement with many of the observed features of Type Ia supernovae (§3). For $\dot{M} = 2.5 \times 10^{-10}\ M_\odot\ \mathrm{yr}^{-1}$, carbon burning is ignited in the *solid* core ($\Gamma > 170$: below the dotted line) when the central density is as high as $\rho_c \sim 10^{10}\ \mathrm{g\ cm}^{-3}$. For comparison, the ignition point of off-center carbon burning is shown for $\dot{M} = 4 \times 10^{-6}\ M_\odot\ \mathrm{yr}^{-1}$.

Accordingly, the ultimate fate of accreting C+O white dwarfs depends on $\dot{M}$ and the inintial mass of the white dwarf M_{CO}, as summarized in Figure 3. $\dot{M}$ denotes the growth rate of the C+O white dwarf mass irrespective of the composition of the accreting matter. A similar diagram for the O+Ne+Mg white dwarfs is shown in Figure 4.

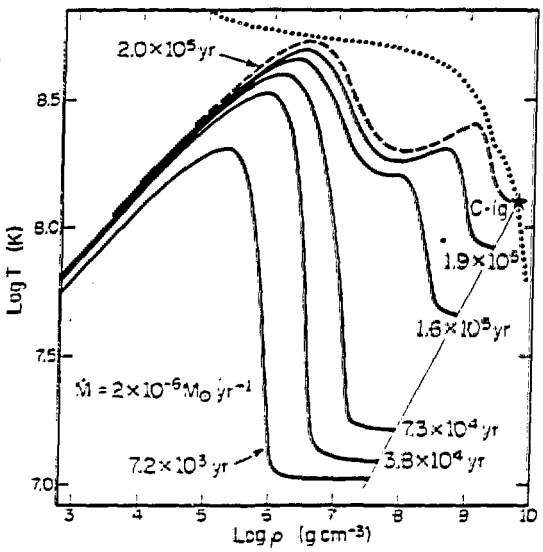

Fig. 1

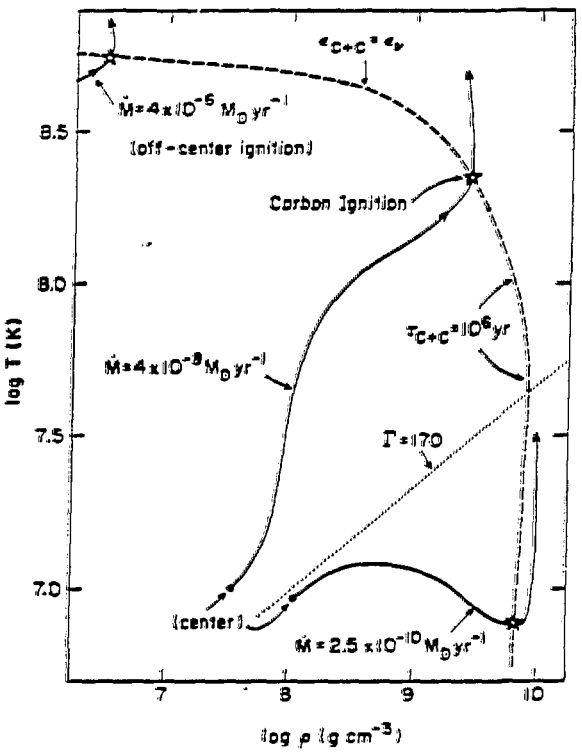

Fig. 2

Figure 1: Structure of the accreting C+O white dwarf in the density - temperature plane as a function of time for the model with $\dot{M} = 2 \times 10^{-6}\ M_\odot\ \mathrm{yr}^{-1}$ and the initial mass of 1.0 $M_\odot$. A heat wave propagates from the hot outer layer to the central region. The thin solid lines shows the adiabat followed by the central point for an initial temperature of 10^7 K. The dotted curve is an approximate ignition line of carbon burnig defined in Figure 2.

Figure 2: Evolutionary path of (ρ_c, T_c) at the center of accreting C+O white dwarfs for two cases. The dashed curve is an approximate ignition line where the rate of carbon burning ϵ_{C+C} is equal to the rate of neutrino losses ϵ_ν for $T > 2 \times 10^8$ K and $\tau_{C+C} \equiv c_p\ T/\epsilon_{C+C} = 10^6$ yr for $T \leq 2 \times 10^8$ K (c_p is the specific heat).

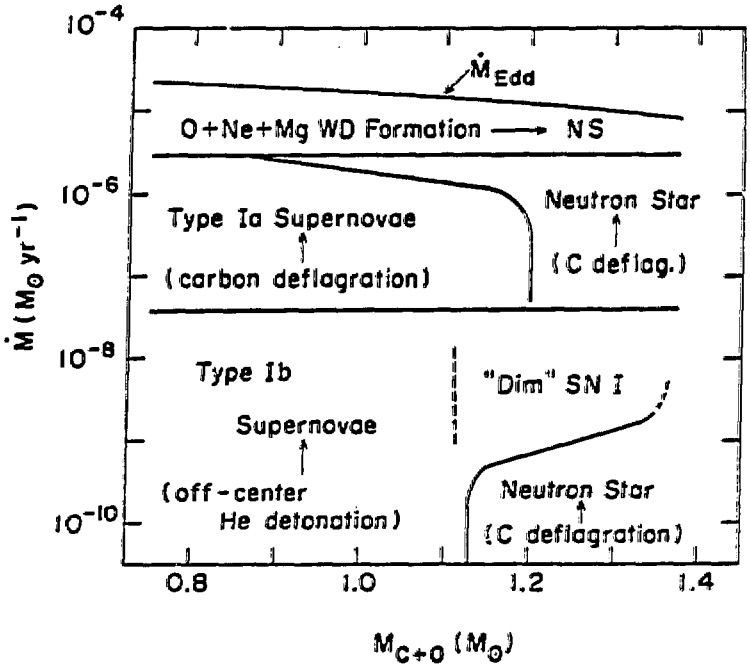

Figure 3: The final fate of accreting C+O white dwarfs expected for their initial mass M_{CO} and accretion rate $\dot{M}$. For two regions in $\dot{M}$ - M_{CO} plane indicated by *Neutron Star*, carbon deflagration is ignited in the center when the density is as high as $\rho_c \simeq 10^{10}$ g cm^{-3}. Propagation of the deflagration wave will induce collapse to form a neutron star. See text for other cases.

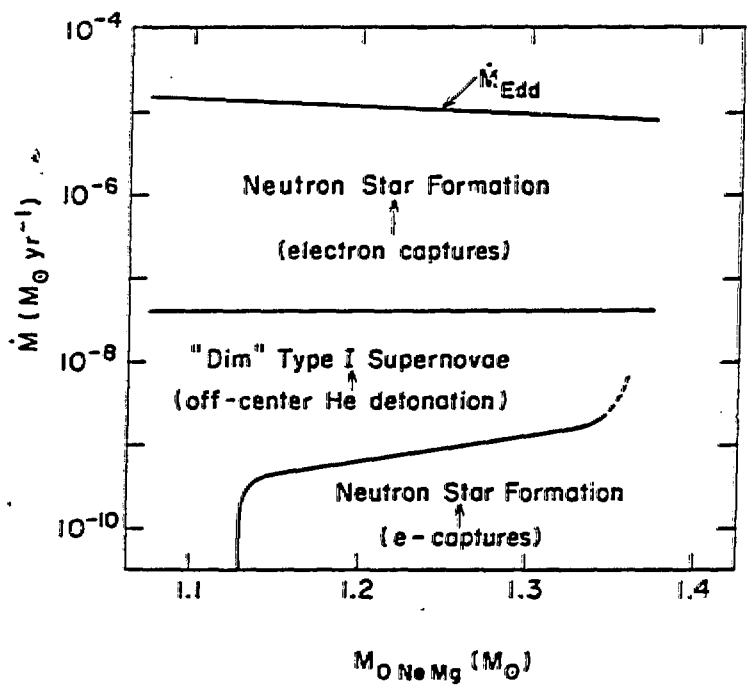

Figure 4: Same as Figure 3 but for O+Ne+Mg white dwarfs. For a wider range of $\dot{M}$ and the initial mass, M_{ONeMg}, neutron star formation triggered by electron capture on ^{24}Mg and ^{20}Ne is expected.

III. MODELS FOR TYPE Ia SUPERNOVAE

3.1 Explosive Nucleosynthesis in Carbon Deflagration Models

For relatively high accretion rates ($2.7 \times 10^{-6}\ M_\odot\ \mathrm{yr}^{-1} > \dot{M} > 4 \times 10^{-8}\ M_\odot\ \mathrm{yr}^{-1}$), a carbon deflagration starts in the white dwarf's center at a relatively low central density ($\rho_c \sim 3 \times 10^9$ g cm^{-3}) (Nomoto, Thielemann, and Yokoi 1984, NTY). The *convective* deflagration wave then propagates outward at a subsonic velocity and incinerates the material of the inner layers to nuclear statistical equilibrium (NSE). When the deflagration wave arrives at the outer layers ($M_r > 0.7\ M_\odot$), the density it then encounters has already decreased below 10^8 g cm^{-3} due to the expansion of the white dwarf (Figure 5). At such densities, the peak temperature, T_p, attained behind the deflagration front is too low to process the material to NSE. The products of explosive nucleosynthesis depend on $T_{p,9} \equiv T_p/10^9$ K, and the density, ρ_p, at the deflagration front and, thus, vary from layer to layer as seen in Figures 6 and 7 (Thielemann, Nomoto, and Yokoi 1986, TNY)

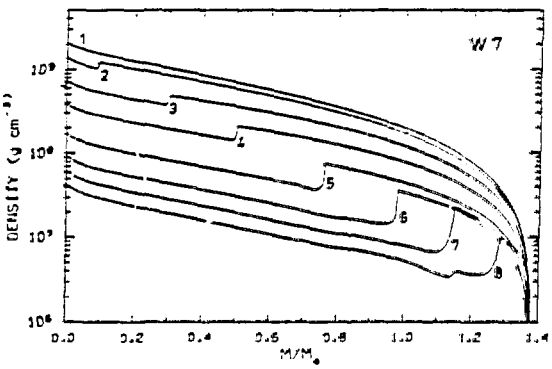

Figure 5: Change in the density distribution during the propagation of the carbon deflagration wave (NTY).

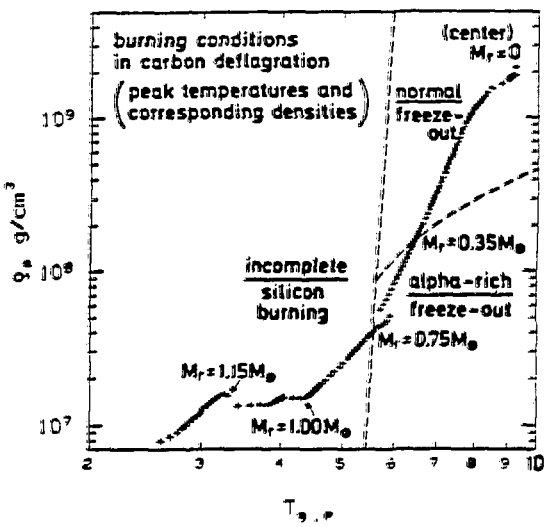

Figure 6: Peak temperatures and densities attained at the deflagration front are indicated by crosses from the center to $M_r = 1.28\ M_\odot$. The dashed lines show the boundaries of various mode of freeze-out (TNY).

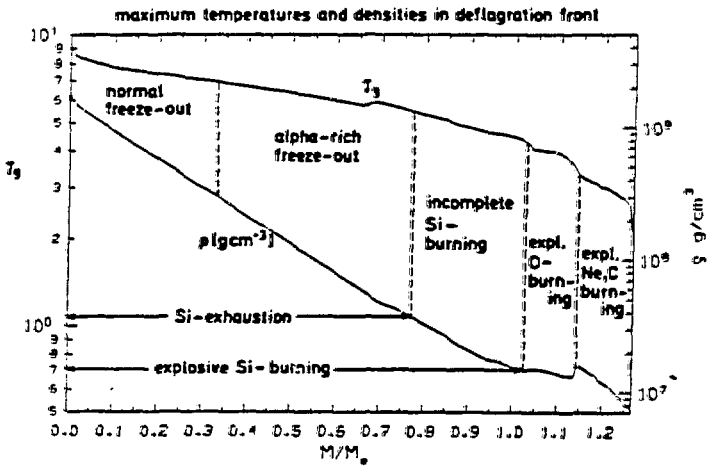

Figure 7: Same as Figure 6 but shown as a function of Lagrangian mass (TNY).

Figure 8 shows the evolution of abundances during the temperature decrease until freeze-out for explosive Si-burning layer ($M_r < 1.0 M_\odot$). Figures 9a-c show nucleosynthesis of oxygen, neon, and carbon, respectively. Some features are:

1) In the center of $M_r < 0.35\ M_\odot$, *normal freeze-out* takes place, i.e., freezing due to deficient α-particles. *Iron peak elements are produced.* Degree of neutronization depends on electron capture mostly on free proton and is very sensitive to the propagation speed of the deflagration wave, especially near the center. In the particular model of NTY, ^{58}Ni is overproduced relative to the solar abundance but it is subject to this uncertainty.

2) For $0.35\ M_\odot < M_r < 0.75\ M_\odot$, the density is too low for the 3α process to complete (*α-rich freezeout*). The α-capture processes, most importantly ^{54}Fe (α,γ) ^{58}Ni, build up heavier nuclei. As a result, the ratio ^{58}Ni /^{54}Fe is significantly larger than that of NSE.

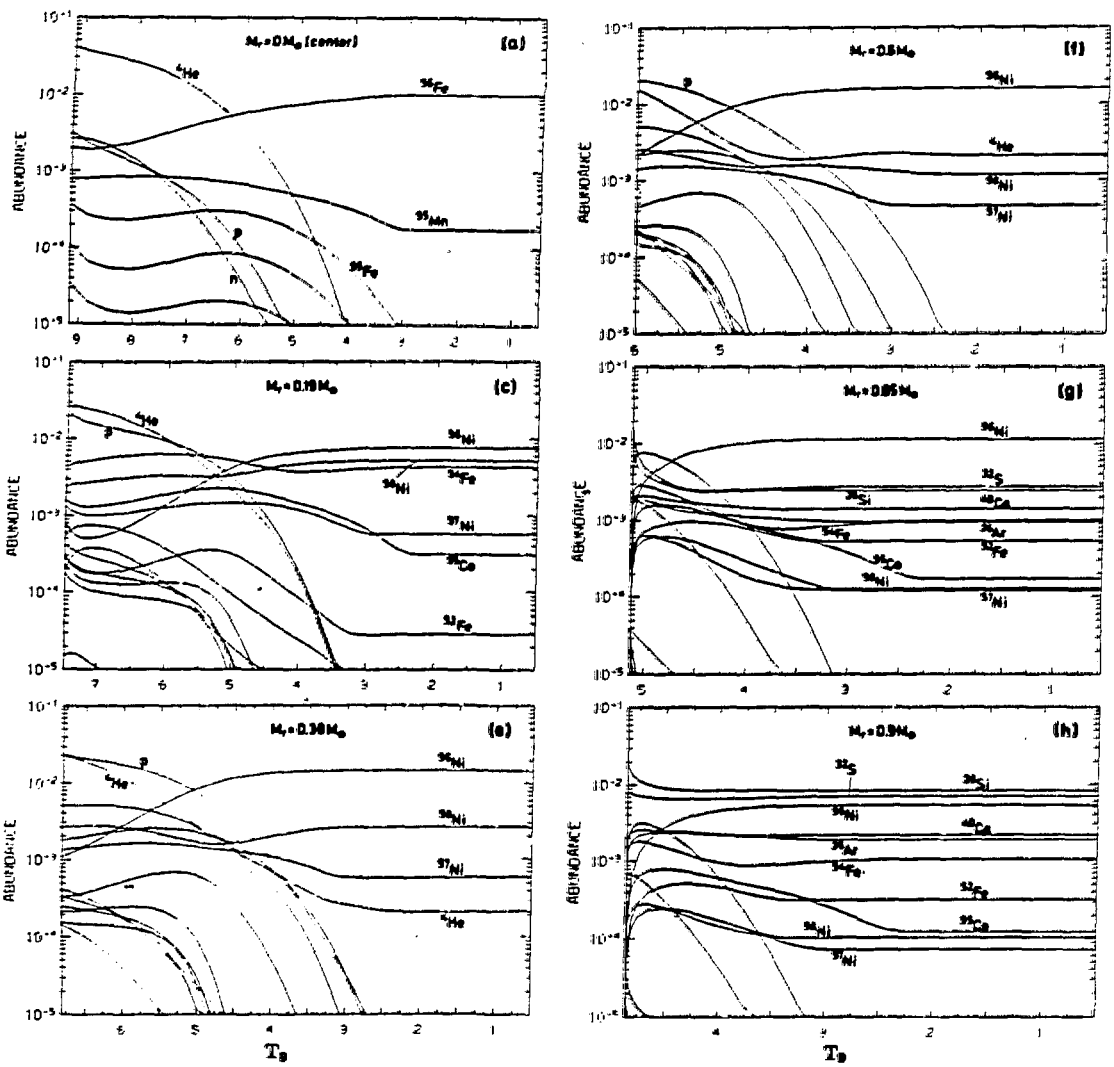

Figure 8: Nucleosynthesis during freeze-out (TNY).

3) For 0.75 - 1.0 $M_\odot$, explosive Si-burning is incomplete and a mixture of ^{56}Ni and Si - S - Ca is produced. The importance of the existence of this layer is discussed in §3.2 in relation with synthetic spectra.

4) In explosive oxygen burning, some ^{54}Fe is produced together with Si, S, Ar, and Ca (Figure 9). This is due to the initial neutron excess originating from ^{22}Ne. Therefore the ^{54}Fe abundance depends on the initial ^{14}N abundance. For Population II white dwarfs, ^{54}Fe would be significantly smaller (Truran et al. 1968). This may be important in view of synthetic spectra (§3.2) as well as nucleosynthesis.

Resulting nucleosynthesis is shown in Figure 10 as a function of M_r. In total, about 0.6 $M_\odot$ of ^{56}Ni is synthesized in this model (NTY). If the deflagration is faster (slower), the amount of ^{56}Ni is larger (smaller). In the outer layers, intermediate mass elements such as Ca, Ar, S, Si are produced. The white dwarf is disrupted completely and no neutron star residue remains (NTY; Woosley et al. 1984).

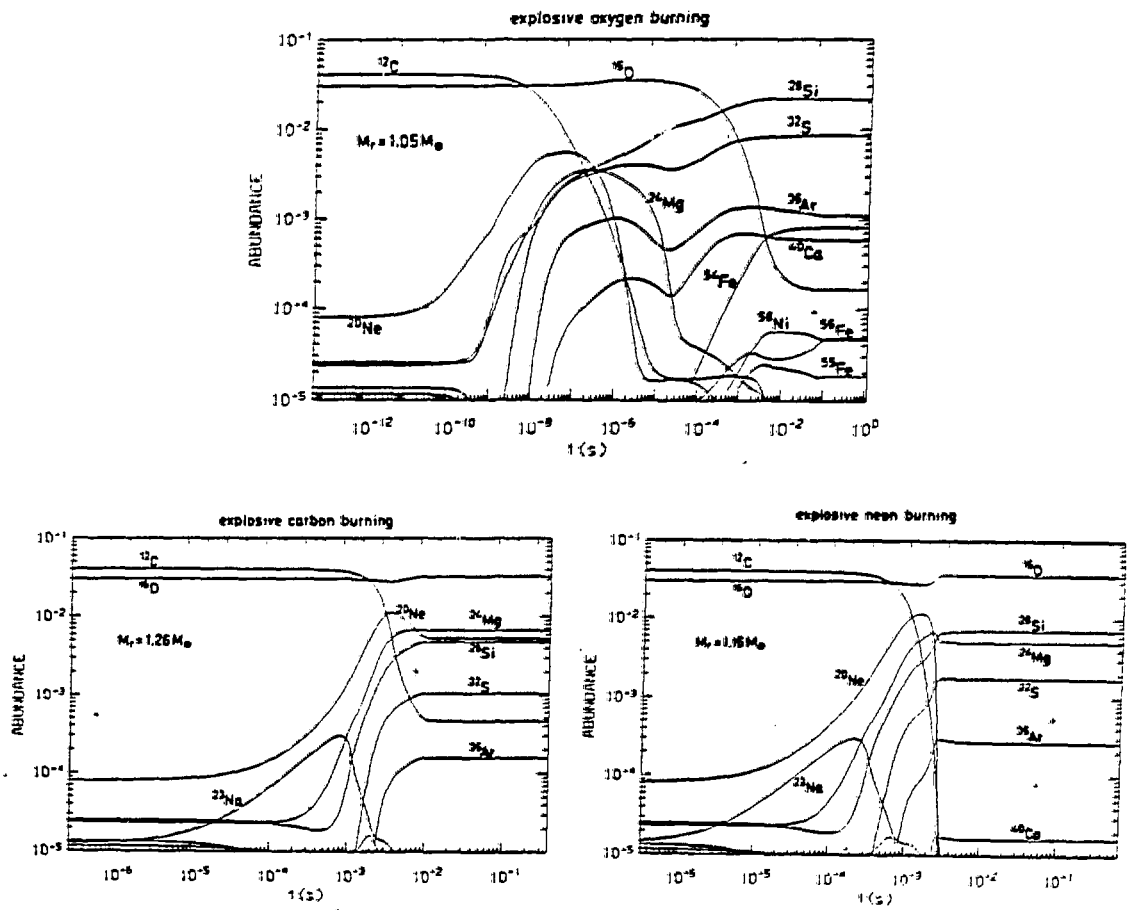

Figure 9: a) Nucleosynthesis in explosive oxygen burning, b) explosive neon burning, and c) explosive carbon burning (TNY).

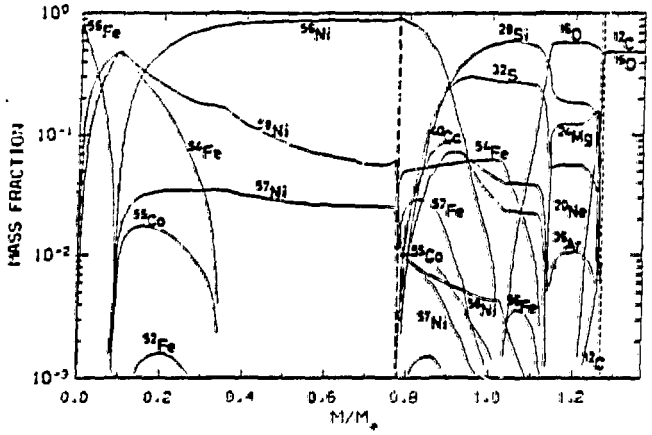

Figure 10: Composition structure after explosive nucleosynthesis in the carbon deflagration wave (NTY). At $M_r < 0.7 M_\odot$, the white dwarf undergoes almost incineration to NSE. At 0.7 $M_\odot < M_r < 1.3$ $M_\odot$, the white dwarf undergoes partial explsive bup. In the outermost layer ($M_r >$ 1.3 $M_\odot$), C+O remain unburned.

3.2 Comparison with Observations

The carbon deflagration model can account for the light curves, early time specta, and late time spectra of Type Ia supernovae as follows (Nomoto 1986a; Woosley and Weaver 1986b):

1) The theoretical light curve based on the radioactive decays of ^{56}Ni and ^{56}Co into ^{56}Fe fits the observations well (Woosley and Weaver 1986b,c). Since Type Ia supernovae are quite uniform, they can be used as a standard candle to determine the distances to the parent galaxies. If we adopt the ^{56}Ni decay model, the maximum brightness of SN Ia is almost proportinal to the ^{56}Ni mass. Then Hubble constant is obtained as (Arnett et al. 1985):

$$H_0 = 46(M_{\rm Ni}/M_\odot)^{-1/2}. \qquad (1)$$

The amount of ^{56}Ni produced is related to the propagation velocity of the deflagration wave and thus subject to uncertainty. We can obtain some constraints on the ^{56}Ni mass from the maximum light spectra as discussed below.

2) The synthetic spectum at maximum light is in excellent agreement with the observed spectum of SN 1981b (Branch et al. 1983) as seen in Figure 11 (Branch et al. 1985; Harkness 1986; Wheeler and Harkness 1986). The feature near 6125 Å is clearly identified as the Si II line that is a signature of Type Ia supernovae (see discussion concerning Type Ib below). To account for the maximum light spectra, materials with a mixture produced by incomplete Si-burning at $M_r = 0.75$ - 1.0 $M_\odot$ (^{56}Ni, ^{40}Ca , and Si - S) need to be conveyed to the surface. Those freshly synthesized Co and Fe should exist near the photosphere expanding at $\sim 10^4$ km s^{-1} (Branch and Venkatakrishna 1986). The expansion velocity of the material at the boundary between complete and incomplete Si-burning gives the slowest velocity for Ca. If the deflagration is significantly slower than the above model and the mass of ^{56}Ni is smaller than $\sim$ 0.5 $M_\odot$, this velocity is lower than the observed lowest value of 8,000 km s^{-1} (Branch et al. 1983) and thus inconsistent with SN Ia. Accordingly the ^{56}Ni mass of 0.5 $M_\odot$ gives the upper limit to $H_0 \simeq 65$ according to Eq.(1). The model which is in good agreement with observed spectra produces 0.58 $M_\odot$ ^{56}Ni which gives $H_0 \simeq 60$ (Nomoto 1986a).

3) At late times, the outer layers are transparent and the inner Ni-Co-Fe core is exposed. Synthetic spectra of emission lines of [Fe II] and [Co I] agree quite well with the spectra observed at such phase (Woosley et al. 1984).

Though several problems remain solved, the synthetic spectra have provided a good evidence that Type Ia supernovae are the explosion of white dwarfs. At the same time, the spectra give important constraints on the nucleosynthesis model.

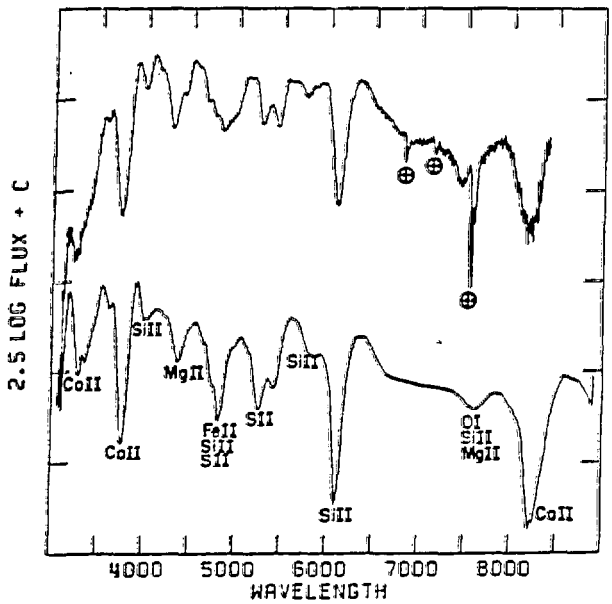

Figure 11: The maximum-light spectrum of SN 1981b (top) is compared to a synthetic spectrum for the carbon deflagration model (NTY) 15 days after the explosion (taken from Branch et al. 1985). In this model outer layer is assumed to be mixed. Terrestrial absorption features in the observed spectrum are indicated.

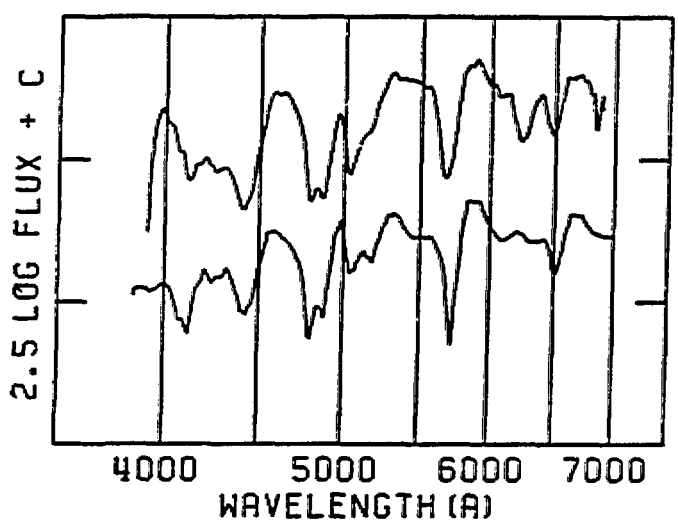

Figure 12: The maximum-light spectrum of the Type Ib SN 1984*l* in NGC 991 (upper) (Wheeler and Levreault 1985) is compared with a synthetic spectrum (lower) based on resonant-scattering lines of He I and Fe II superimposed on a continuum (taken from Branch and Nomoto 1986). In the synthetic spectrum the blueshifted absorption component of He I λ6678 appears near 6500 Å and He I λ5876 appears near 5850 Å. Other features are produced primarily by Fe II lines.

IV. MODELS FOR TYPE Ib SUPERNOVAE

4.1 Wolf-Rayet Star Model

Recent observations indicate that there exists another kind of Type I supernovae, designated Type Ib (SN Ib) (e.g., Wheeler and Harkness 1986 and references therein). The SN Ib spectra lack hydrogen lines (definition of SN I) and are characterized by both the lack of the 6125 Å Si feature at maximum-light spectra and the appearance of oxygen emission lines at late times (Gaskel et al. 1986; Fillipenko and Sargent 1985). More than 5 $M_\odot$ (Begelman and Sarazin 1986) and as much as 15 $M_\odot$ (Gaskel et al. 1986) of oxygen has been inferred from the late time spectra. Moreover, SN Ib have been seen in only spiral galaxies, usually in their star-forming regions. These signatures have led to the currently popular idea that the progenitors of SN Ib are Wolf-Rayet stars (Wheeler and Levreault 1985; Gaskel et al 1986; Begelman and Sarazin 1986; Chevalier 1986). However, such a large mass of oxygen may yield a theoretcal light curve whose decline is too slow to be compatible with SN Ib observations (Wheeler and Levrerault 1985; Woosley 1986). In addition, Wolf-Rayet death rates and the SN Ib frequency might be incompatible.

4.2 White Dwarf Model

Branch and Nomoto (1986) have suggested that the observed spectra are better explained by an accreting white dwarf model. In Figure 12, the maximum-light spectrum of SN 1984*l* is compared with a synthetic spectrum. The expansion velocity of matter at the photosphere is assumed to be 8,000 km s^{-1}. Two of the absorption lines in the red are identified as He I lines (Wheeler and Harkness 1986) and other features are well explained as Fe II lines. In addition, ultraviolet features can fit with a synthetic spectrum of Co II and Fe I lines if the photoshperic velocity is 12,000 km s^{-1} (Branch and Venkatakrishna 1986). The above interpretation of the early spectrum together with the presence of the oxygen lines in the late time spectrum suggests that Fe, Co (decaying), and He are in the outer high-velocity layers and that oxygen and some other intermediate mass elements are in the inner layers. In other words, the composition structure of SN Ib's appears to be that for SN Ia's inverted.

The existence of such high velocity Fe and, especially, Co is difficult to explain with the Wolf-Rayet model (see, however, Wheeler et al. 1986 for the interpretaion of Fe). Branch and Nomoto (1986) have speculated that the progenitors of SN Ib differ from the progenitors of SN Ia in having a lower accretion rate, i.e., $\dot{M} < 4 \times 10^{-8}$ $M_\odot$ yr^{-1}. For such low accretion rates, the helium shell flash grows into a detonation. The outcome may be more like a *single* detonation than the double detonation obtained in the spherical calculations (Nomoto 1982b; Woosley et al. 1986) because the off-center flash will occur at a point rather than all over a spherical shell. The outer helium layer will burn to mostly ^{56}Ni with a trace He and be ejected into space. The inner C+O core will remain unburned due to non-spherical effects and a part or most of the C+O will be ejected. Since the ejected mass of ^{56}Ni will be as small as 0.1 - 0.3 $M_\odot$, the peak luminosity of this model is lower than that for SN Ia by a factor of 2 - 6. This result is consisttent with the observations of SN Ib.

This *single* detonation scenario requires that $\dot{M}$ be lower than that needed for the carbon deflagration model of SN Ia. This requirement may be inconsistent with the relatively *young* character of SN Ib. However, if the white dwarf accretes matter with an efficiency of only 0.03 - 0.1 (Davidson and Ostriker 1973) from a wind (10^{-6} - 10^{-7} $M_\odot$ yr^{-1}) of a relatively massive (4 - 7 $M_\odot$) red giant companion (Iben and Tutukov), the model would be consistent. Further, this scenario is consistent with the radio observations of SN Ib in that they can be explained by the interaction of supernova ejecta with the circumstellar shell (Panagia et al. 1986; Sramek et al. 1984; Chevalier 1984).

Both Wolf-Rayet and white dwarf models for SN Ib should be tested by quantitative comparison with observations based on theoretical light curves, synthetic spectra, and multi-dimensional hydrodynamical calculatons of off-center detonations.

4.3 Dim Type I Supernovae

If an off-center *single* detonation occurs on a very massive white dwarf ($> \sim 1.1\ M_\odot$), the resulting supernova will be rather *dim*, because the accumulation of only a small amount of helium (~ 0.01 - $0.1\ M_\odot$) can lead to the helium detonation (Fujimoto and Sugimoto 1982). In most cases, an unburned C+O core will be left behind as a white dwarf. Such dim supernovae (Branch and Doggett 1985) are more likely to be associated with O+Ne+Mg white dwarfs since their masses are larger than $\sim 1.2\ M_\odot$.

V. COLLAPSE INDUCED BY CARBON DEFLAGRATION AT HIGH DENSITY

5.1 Carbon Ignition at High Density

As discussed in §2, there are two scenarios in which a carbon deflagration is initiated in the center when the central density is as high as 10^{10} g cm^{-3}. The corresponding region of parameter space is indicated by *Neutron Star* in Figure 3 where neutron star formation by white dwarf collapse is expected. The evolution of the white dwarfs in these two regions is summarized as follows:

1) For $2.7 \times 10^{-6}\ M_\odot\ \mathrm{yr}^{-1} > \dot{M} > 4 \times 10^{-8}\ M_\odot\ \mathrm{yr}^{-1}$ and $M_{CO} > 1.2\ M_\odot$, a central density as high as 10^{10} g cm^{-3} is reached by adiabatic compression if the white dwarf is sufficiently cold at the onset of accretion (Canal and Isern 1980). For $\dot{M} > 10^{-6}\ M_\odot\ \mathrm{yr}^{-1}$, the lower mass limit is not $1.2\ M_\odot$, but $1.0\ M_\odot$ (Nomoto and Iben 1985). An example of such an evolution is given in Figure 1, where $\dot{M} = 2 \times 10^{-6}\ M_\odot\ \mathrm{yr}^{-1}$ (Nomoto and Iben 1985).

2) For $\dot{M} \leq 10^{-9}\ M_\odot\ \mathrm{yr}^{-1}$ and $M_{CO} > 1.13\ M_\odot$, the white dwarf is too cold to initiate a helium detonation. Eventually pycnonuclear carbon burning starts in the center when ρ_c reaches $\sim 10^{10}$ g cm^{-3}. An evolutionary path of ρ_c - T_c for a model with $\dot{M} = 2.5 \times 10^{-10}\ M_\odot\ \mathrm{yr}^{-1}$ and $M_{CO} = 1.16\ M_\odot$ is shown in Figure 2. In this model, the outer layer of $0.24\ M_\odot$ is composed of helium.

5.2 Conductive Deflagration

At densities as high as 10^{10} g cm^{-3}, the carbon deflagration may not lead to an explosion since electron capture is much faster at these high densities than at the lower densities encountered in the models of SN Ia. Moreover, if the central part of the white dwarf is in the solid state, the propagation mode of the burning front could be different. If the solid is strong enough, convection will be suppressed and the burning front will propagate as a *conductive* deflagration wave (Canal and Isern 1979; Isern et al. 1983) though more study is needed on this point. The propagation velocity of a conductive deflagration wave is given approximately by the expression, $v_{def} \sim \delta/\tau_n \sim (\sigma/c_v\tau_n)^{1/2}$, where δ denotes the width of burning front, τ_n the nuclear burning timescale, σ the conductivity, and c_v the specific heat (Buchler et al. 1980; Woosley and Weaver 1986c). This gives $v_{def} \sim 100$ km s^{-1} at $\rho \sim 10^{10}$ g cm^{-3}, which is about 0.01 v_s (Woosley and Weaver 1986c). Here v_s is the sound speed, equal to 1.0 - 1.3×10^4 km s^{-1} between $\rho = 10^9$ - 10^{10} g cm^{-3}.

Whether the white dwarf explodes or collapses depends on whether, behind the deflagration wave, nuclear energy release or electron capture is faster. A white dwarf whose mass is close to the Chandrasekhar mass has an adiabatic index close to 3, so that even a small energy release can cause substantial expansion (Woosley and Weaver 1986c). However, a slight pressure decrease due to electron capture will easily induce collapse. If v_{def} is low (high) enough and/or the central density is high (low) enough, a carbon deflagration will lead to collapse (explosion). The outcome is rather sensitive to v_{def} and the central density.

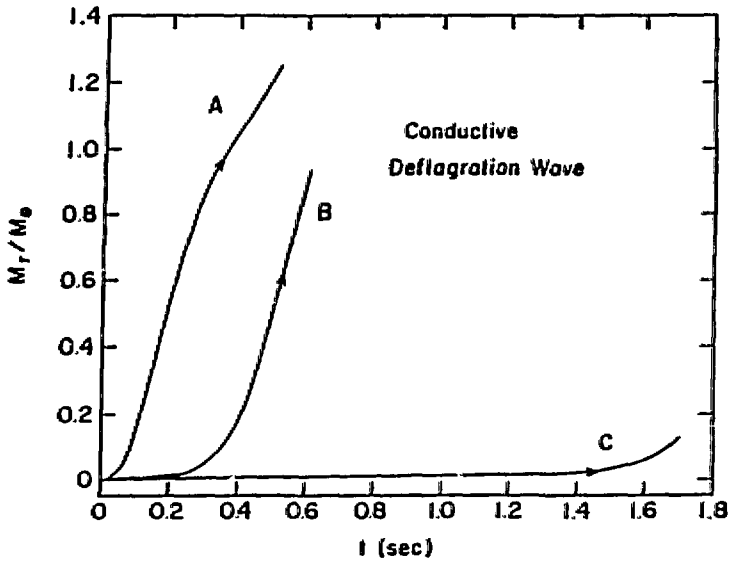

Figure 13: Propagation of the conductive deflagration wave. The location (M_r) of the deflagration front is shown as a function of time, t, for three cases (A, B, C) of parametrized conductivity.

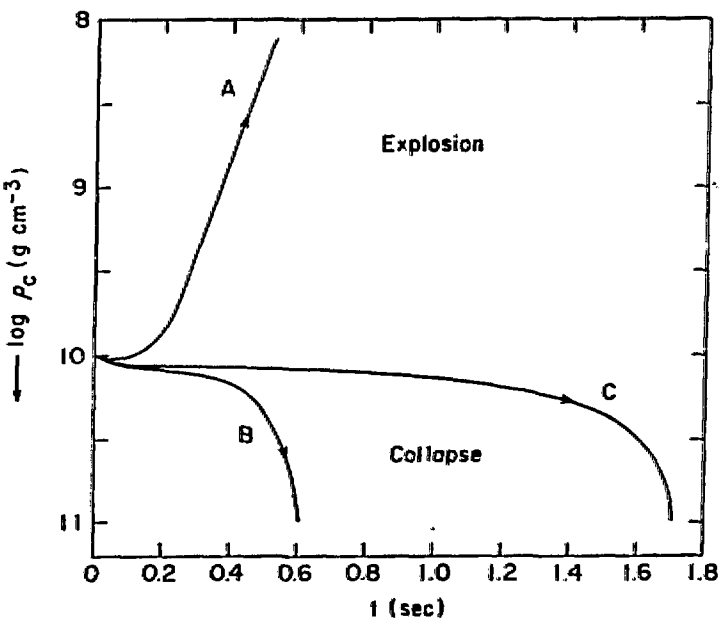

Figure 14: Change in the central density of the white dwarf associated with the propagation of the conductive deflagration wave. Relatively slow propagation in Cases B and C leads to the increase in ρ_c, i.e., collapse of the white dwarf. On the other hand, faster proapagation in Case A induces the explosion of the white dwarf.

We have performed numerical simulations of a conductive deflagration started at high central density ($\rho_c \simeq 10^{10}$ g cm^{-3}), with $\dot{M} = 2.5 \times 10^{-10}\ M_\odot$ yr^{-1} and $M_{CO} = 1.16\ M_\odot$, as shown in Figure 2 (Nomoto 1986b). Here $X_C = X_O = 0.5$ and we have assumed that no chemical separation occurs. Pycnonuclear carbon burning commences in the solid region and turns into thermonuclear runaway as a result of the temperature rise. Throughout the simulation, convection is neglected.

The actual simulation of a conductive deflagration requires extremely fine zoning (Woosley and Weaver 1986c). Instead of employing a grid whose fineness would slow the calculations unduly, we have parametrized the conductivity to obtain a range of reasonable v_{def}. With these, we have explored the range of possible hydrodynamical responses of the white dwarf. In Figure 13, the location of the deflagration front as a function of time, t, after initiation is plotted for three cases (A, B, C). In addition, Case D of the slowest propagation has been calculated. The average v_{def}/v_s for Cases A, B, C, and D is about 0.15, 0.1, 0.06, and 0,01, respectively. In Figure 14, the evolution of the central density, ρ_c, for Cases A - C is plotted.

5.3 Cases of Collapse

As Figure 14 indicates, in Case B, the central density increases as the deflagration front propagates outward. When the deflagration front has reached $M_r \simeq 0.9\ M_\odot$ ($t \simeq 0.6$ s), ρ_c is as high as 10^{11} g cm^{-3}. Clearly, the white dwarf now undergoes quasi-dynamic contraction (not yet free-fall collapse) because electron capture on NSE elements rapidly reduce the electron mole number, Y_e, behind the deflagration wave. This effect dominates the opposing effect of nuclear burning. In the central region of $\rho_c \simeq 10^{10}$ g cm^{-3}, typical values of τ_{ec} ($\equiv Y_e/|\dot{Y}_e|$) are 0.06 s and 0.16 s for $Y_e \simeq 0.5$ and 0.47, respectively. At $t = 0.16$ s, Y_e has dropped to 0.42 at the center. Because of the decrease in the electron capture rate in the central region, electron capture is fastest at the deflagration front and thus the density there is important. In Case B, the density at the front is gradually decreasing but is still as high as 4×10^9 g cm^{-3} at $M_r = 0.9\ M_\odot$, and τ_{ec} is as short as $\simeq 0.3$ s (at $Y_e = 0.5$). Moreover, once the contraction of the white dwarf begins, photodissociation becomes important, further promoting collapse.

In Case C, the contraction is much more gradual than in Case B because the deflagration wave is slower. When ρ_c reaches 10^{11} g cm^{-3}, the burned mass is only $0.13\ M_\odot$ (Figs. 13 and 14).

In Case D, for which v_{def} ($\sim 0.01\ v_s$) is close to the actual conductive deflagration speed, it takes 155 s to reach $\rho_c \simeq 10^{11}$ g cm^{-3}. At $t = 155$ s, the mass of the burned region is only $0.03\ M_\odot$ and $Y_e \sim 0.39$.

5.4 Case of Explosion

On the other hand, in Case A, ρ_c decreases as the deflagration propagates outward. By the time the front has reached $M_r \simeq 1.2\ M_\odot$, the total energy of the white dwarf is already 1.2×10^{51} ergs and it is clear that it will be completely disrupted. Nuclear energy release dominates electron capture because the front's density, and hence its electron capture rate, decreases as the front propagates outward. The expansion of the burned core of the white dwarf decreases the density and temperature of the entire star. Once this expansion is substantial, it is impossible for electron capture to induce reimplosion. Only for initial central density as high as 3×10^{10} g cm^{-3}, similar to those in the detonation case (Bruenn 1972; Mazurek et al. 1974), would reimplosion be a possible outcome.

Because of the expansion, when the deflagration front has reached $M_r = 1.0$ - $1.16\ M_\odot$, its density is as low as 10^8 - 10^7 g cm^{-3}. Therefore, some intermediate mass elements, such as Ca, Ar, S, and Si, are synthesized (NTY). When the deflagration wave arrives at the base of helium layer ($M_r = 1.16\ M_\odot$), it turns into a helium detonation because helium has a large Q-value and a low ignition temperature. Despite the expansion of the white dwarf, detonation wave does not die and it processes most of the matter to ^{56}Ni. Were it not for the Ca - Si layer sandwiched between the two ^{56}Ni layers, the final outcome for Case A would be similar to the outcome for the double detonation supernovae (Nomoto 1982b; Woosley et al. 1986) where both carbon and helium layers are burned to ^{56}Ni. This type of supernovae should not be very frequent since they eject too much neutron-rich iron peak matter into the Galaxy (Nomoto et al. 1984a).

5.5 Convective Deflagration

If carbon ignition at high densities occurs for $\dot{M} > 4 \times 10^{-8}\ M_\odot\ \mathrm{yr}^{-1}$ and $M_{CO} > 1.2\ M_\odot$, adiabatic compression may have already melted the solid core when carbon is ignited. Convective deflagration would then develope, though conductive deflagration could still dominate in the central region (Woosley and Weaver 1986c). Even for the solid core, propagation of the deflagration wave is not necessarily due to conduction alone since convection could influence the melting the solid core (Mochkovitch 1980). To investigate these cases, a set of numerical experiments has been performed with the above model, but under the assumption that the deflagration wave is propagating by convection in fluid layers. Our treatment of convection is the same as that employed in NTY, i.e., Unno's (1967) time-dependent mixing length theory with a parameter $\alpha = \ell / H_p$ where ℓ is the mixing length and H_p is the pressure scale height.

For $\alpha = 0.7$, the propagation velocity is as slow as $v_{def}/v_s \sim 0.06$, 0.09, and 0.11 when the deflagration reaches $M_r/M_\odot = 0.2$, 0.4, and 0.6, respectively. As expected, the white dwarf collapses as in Case B. On the other hand, for $\alpha = 1.0$, $v_{def}/v_s \sim 0.10$, 0.15, and 0.20 at $M_r/M_\odot = 0.2$, 0.4, and 0.6, respectively, and the white dwarf explodes completely. Since a value for α of 0.7 is preferred in the low density carbon deflagration model of SN Ia (§3), a plausible choice for α in the present context may be 0.7, not 1.0. (For both low and high central densities, the carbon deflagration with $\alpha = 1.0$ grows into a *detonation* in the outer layer and incinerates almost the entire star to the iron peak. This is incompatible with observations of SN Ia (NTY). Therefore, for plausible choices of the α parameter, a carbon deflagration initiated at high densities will result in white dwarf collapse, not explosion.

VI. THE FATE OF DOUBLE WHITE DWARFS

Though the carbon deflagration model can account for many of the observed features of Type Ia supernovae, the exact progenitor binary system is difficult to identify because binary star evolution, especially its common envelope phase, is very complex. In the efforts to construct the likely scenario for precursor system, Iben and Tutukov (1984) and Webbink (1984) have concluded that many intermediate mass binary system will end up as double degenerates and that the C+O - C+O white dwarf pair is the most likely candidate for SN I precursor (see Iben 1986 for recent development).

When the smaller mass white dwarf filles its Roche lobe, merging process starts. The evolution of the more massive component has been simulated as a rapid mass accretion for the C+O - C+O white dwarf pair (Nomoto and Iben 1985; Saio and Nomoto 1985; Woosley and Weaver 1986a), and the He - He pair (Saio and Nomoto 1986).

6.1 He - He White Dwarf Pair

The following is the summary of the preliminary calculation by Saio and Nomoto (1986). The initial mass and luminosity of the helium white dwarf are 0.4 $M_\odot$ and 1.9×10^{-3} $L_\odot$ ($T_c = 1 \times 10^7$ K) and the mass accretion rate is $\dot{M} = 1 \times 10^{-7}$ $M_\odot\ \mathrm{yr}^{-1}$. As discussed in §2, mass accretion first heats up the surface layer as seen from the temperature distribution in Figure 15. The stage numbers correspond to 1: 5×10^4 yr, 2: 3.1×10^5 yr, 3: 1.0×10^6 yr after the onset of accretion. When the white dwarf mass reaches 0.515 $M_\odot$ (stage 4 in Figure 16), helium ignites at $M_r = 0.434\ M_\odot$. Afterwards helium burning front propagates inward due to heat conduction as seen in Figure 16. Here the stage numbers correspond to 4: off-center ignition, 5: 2.3×10^4 yr, 6: 9.1×10^4 yr, 7: 4.1×10^5 yr, and 8: 1.5×10^6 yr after the off-center ignition. At stage 8, helium burning front reaches the center.

During the propagation, helium burning makes a series of mild flashes. The first flash is the strongest (the nuclear energy generation rate is $L_n \simeq 4 \times 10^9$ $L_\odot$ at its peak) and getting weaker as the front moves inward. When the front reaches the center, $L_n \simeq 60\ L_\odot$ at the peak. Because of weak electron degeneracy, the flash ceases when only 10 percent of helium is burned. Total nuclear energy released by burning about 10 percent of helium amounts to $\sim 5 \times 10^{49}$ erg. About half of it is radiated away and the rest is used to lift the electron degeneracy.

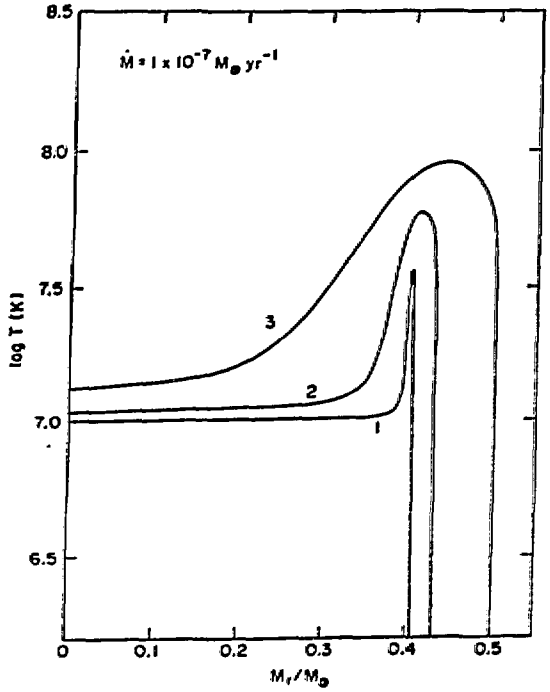

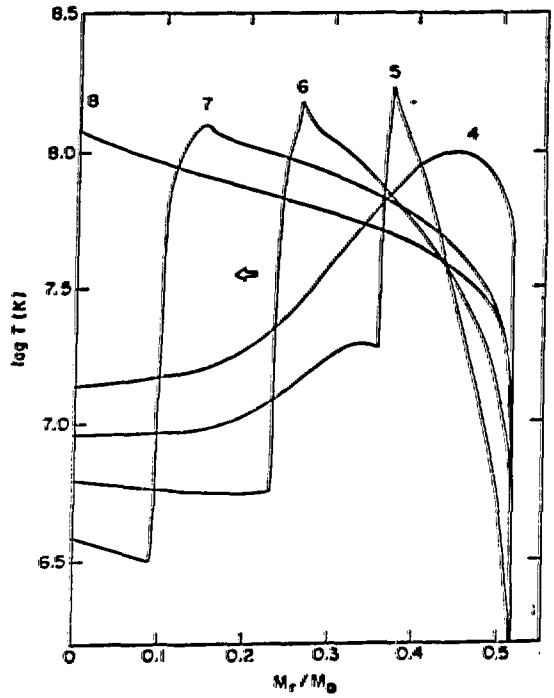

Figure 15 (left): Change in the temperature distribution in the helium white dwarf during accretion phase. Here $\dot{M} = 1 \times 10^{-7}\ M_\odot\ yr^{-1}$ and the initial mass is 0.4 $M_\odot$.

Figure 16 (right): Same as Figure 15 but during the propagation of the burning front.

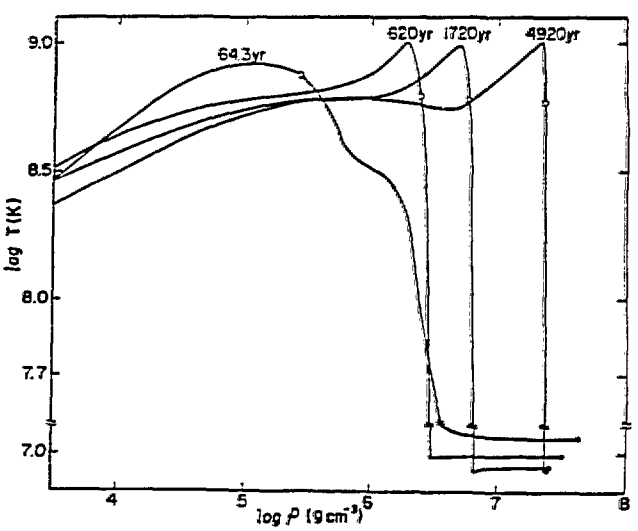

Figure 17 (upper): Propagation of the carbon burning front in the C+O white dwarf. Change in the temperature distribution against the density is shown.

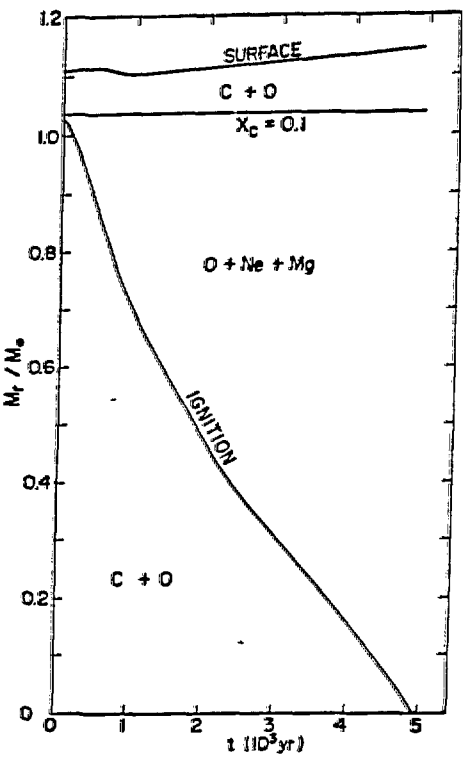

Figure 18 (right): Same as Figure 17 but shown in the M_r - t plane.

After the burning front reaches the center, the helium star undergoes steady burning like a helium-main-sequence star. The steady burning phase lasts 5×10^7 yr and consumes helium in the convective core. Our conclusion is that the merging He - He white dwarf pair changes into a helium-main-sequence star of mass 0.5 - 0.6 $M_\odot$ which will end up as a C+O white dwarf. This is the common fate of accreting helium white dwarfs, as far as the accretion rate is higher than 4×10^{-6} $M_\odot$ yr^{-1} for which an off-center helium flash is ignited (Nomoto and Sugimoto 1977).

6.2 C+O - C+O White Dwarf Pair

The evolution is essentially similar to the above case. In the following example, the initial mass of the C+O white dwarf is 1.0 $M_\odot$ and $\dot{M} = 1 \times 10^{-5}$ $M_\odot$ yr^{-1}. The off-center carbon burning is ignited when $M = 1.11$ $M_\odot$ (Nomoto and Iben 1985) and the burning front propagates inward as a sequence of mild shell flashes as seen in Figures 17 and 18 (Saio and Nomoto 1985, 1986). There are some important differences from the off-center helium burning. First the carbon flash is strong enough to convert all carbon into O+Ne+Mg because of larger white dwarf mass and electron degeneracy. Secondly the temperature at the burning layer is higher and hence most of the nuclear energy is carried away by neutrinos and not used to lift the electron degeneracy. Therefore, when the carbon burning front reaches the center, no carbon is left and the C+O white dwarf is completely converted into an O+Ne+Mg white dwarf. This is always the case for $\dot{M} > 2.7 \times 10^{-6}$ $M_\odot$ yr^{-1} irrespective of the initial model (Kawai et al. 1986). If the accretion is slower, carbon ignites at the center. Then the outcome is either a Type Ia supernova or collapse to form a neutron star depending on the condition discussed in §3 and §5.

The above models assume spherical symmetry which might be a too simple model. We need 3-dimensional hydrodynamical calculation for the mass transfer (see Hachisu et al. 1986a, b) and at leaset 2-dimensional calculation for the propagation of the burning front to know whether the double degenerates are actually Type Ia supernova precursor.

VII. CONCLUDING REMARKS AND DISCUSSION

We have shown how the fate of accreting white dwarfs depends on the initial mass, composition, and age of the white dwarf and accretion rate. In particular, we have examined the critical condition for which a carbon deflagration leads to collapse. If a carbon deflagration is initiated in the center of the white dwarf when $\rho_c \simeq 10^{10}$ g cm^{-3} and if the propagation velocity of the deflagration wave is slower than a certain critical speed, v_{crit}, the outcome is collapse, not explosion. For $v_{def} > v_{crit}$, complete disruption results (and the ejecta contain too much neutron-rich matter). The value of v_{crit} depends on ρ_c at carbon ignition. For $\rho_c \simeq 1 \times 10^{10}$ g cm^{-3}, $v_{crit} \sim 0.15\ v_s$. A lower ρ_c implies a lower v_{crit}. Below a certain critical density, even extremely slow deflagrations results in explosions. In our case of $\rho_c \simeq 1 \times 10^{10}$ g cm^{-3}, for both conductive and convective deflagrations $v_{def} < v_{crit}$ and, therefore, collpase will result.

Such a high central density is reached in two regions of the $\dot{M}$ - M_{CO} plane of Figure 3. One is defined by $\dot{M} > 4 \times 10^{-8}$ $M_\odot$ yr^{-1} and $M_{CO} > 1.2$ $M_\odot$, while the other is defined by $\dot{M} < 10^{-9}$ $M_\odot$ yr^{-1} and $M_{CO} > 1.13$ $M_\odot$. The frequency of such systems may be small. First, if hydrogen-rich matter accretes at $\dot{M} < 10^{-9}$ $M_\odot$ yr^{-1}, nova-like explosions will prevent the white dwarf mass from growing. The hydrogen flash can be avoided if the companion star is a helium star. Secondly, massive C+O white dwarfs (> 1.2 $M_\odot$) may be rare. The formation of such white dwarfs might be prevented if the precursor star lost its hydrogen-rich envelope by either a stellar wind or Roche-lobe overflow before its degenerate C+O core could grow substantially.

As seen in Figure 4, the accretion-induced collapse is the outcome for a wider range of parameter space for O+Ne+Mg white dwarfs. The initial mass of the white dwarf, M_{ONeMg}, is larger than $\sim 1.2\ M_\odot$ (Nomoto 1984a). In many cases, M_{ONeMg} is very close to the Chandrasekhar mass, so that only a small mass increase is enough to trigger collapse. However, an O+Ne+Mg white dwarf is formed from an 8 - 10 $M_\odot$ star. The number of such systems may be significantly smaller than the number of systems containing C+O white dwarfs whose precursors are 1 - 8 $M_\odot$ stars, perhaps, by four order of magnitude (Iben and Tutukov 1984). Even so, the number of low mass X-ray binaries is much smaller than the number of SN I and the statistics may be consistent (Webbink et al. 1983).

A hydrodynamical calculation of such a white dwarf collapse has not been carried out so that we don't know whether mass is ejected. Even if no mass is ejected, a neutron star will be formed because the residue's mass (1.4 $M_\odot$ (baryon mass), $\sim 1.3\ M_\odot$ (gravitational mass)) is smaller than the maximum mass of a neutron star. Nevertheless, it is important to know whether some mass is ejected by the bounce shock and, if mass is ejected, what its composition is. If some ^{56}Ni is ejected, the white dwarf collapse can be observed as a *dim* Type I supernova. Otherwise, the collapse would be *silent*, because most of the explosion energy would go into the kinetic energy of expansion. The interior temperatures would be *too* low to produce a significant optical light curve. If the shock wave is strong enough, some neutron-rich species will be ejected. This might be an important site of some neutron-rich isotopes (Hartman et al. 1985; Takahashi et al. 1986). Mass ejection will affect the binary evolution after the explosion and the results can be compared to the observed neutron star binary systems (e.g., Taam and van den Heuvel 1986).

ACKNOWLEDGEMENT

It is a pleasure to thank Drs. S.H. Kahana, G.E. Brown, A. Yahil, and A. Burrows for useful discussion and hospitality during my stay in Brookhaven and Stony Brook. I would like to thank Drs. D. Branch, J.C. Wheeler, R. Harkness, and Z. Barkat for informative discussion on Type I supernovae during my visit to Univ. of Oklahoma and Texas. This work has been supported in part by the U. S. Department of Energy under Contract No. DE-AC02-76CH00016 and by the Japanese Ministry of Education, Science, and Culture through research grant Nos. 59380001 and 60540152.

REFERENCES

Arnett, W.D., Branch, D., and Wheeler, J.C. 1985, *Nature*, *314*, 337.
Begelman, M.C., and Sarazin, C.L. 1986, *Ap. J. (Letters)*, *302*, L59.
Branch, D., and Doggett, J.B. 1985, *A. J.*, *270*, 2218.
Branch, D., Doggett, J.B., Nomoto, K, and Thielemann, F.-K. 1985, *Ap. J.*, *294*, 619.
Branch, D., Lacy, C.H., McCall, M.L., Sutherland, P.G., Uomoto, A., Wheeler, J.C., and Wills, B.J. 1983, *Ap. J.*, *270*, 123.
Branch, D., and Venkatakrishna, K.L. 1986 *Ap. J. (Letters)*, *306*, L21.
Branch, D., and Nomoto, K. 1986, *Astr. Ap.*, in press.
Bruenn, S.W. 1972, *Ap. J. Suppl.*, *24*, 283.
Buchler, J.R., Colgate, S.A., and Mazurek, T.J. 1980, *J. de Phys. Suppl. 3*, *41*, C2-159.
Canal, R., and Isern, J. 1979, in *IAU Colloquim 53, White Dwarfs and Variable Degenerate Stars*, ed. H.M. Van Horn and V. Weidemann (Rochester: Univ. of Rochester), p.52.
Chevalier, R.A. 1984, *Ap. J. (Letters)*, *285*, L63.
————. 1986, *Highlights of Astronomy*, in press.
Davidson, K., and Ostriker, J.P. 1973, *Ap. J.*, *179*, 585.
Filippenko, A.V., and Sargent, W.L.W. 1985, *Nature*, *316*, 407.
Fujimoto, M.Y., and Sugimoto, D 1982, *Ap. J.*, *257*, 291.
Gaskell, C.M., Cappellaro, E., Dinerste in, H., Garnett, D., Harkness, R.P., and Wheeler, J.C. 1986, *Ap. J. (Letters)*, *306*, L77.
Hachisu, I., Eriguchi, Y., and Nomoto, K. 1986a, *Ap. J.*, *308*, in press.
————. 1986b, *Ap. J.*, *311*, in press.
Harkness, R.P. 1986, in *IAU Colloquium 89, Radiation Hydrodynamics in Stars and Compact Objects*, ed. D. Mihalas and K.H. Winkler (Dordrecht: Reidel), in press.

Hartmann, D., Woosley, S.E., and El Eid, M.F. 1985, *Ap. J., 297*, 837.
Iben, I. Jr. 1986, this volume.
Iben, I. Jr., and Tutukov, A.V. 1984, *Ap. J. Suppl., 54*, 335.
Isern, J., Labay, J., Hernanz, M., and Canal, R. 1983, *Ap. J.., 273*, 320.
Isern, J., Labay, J., and Canal, R. 1984, *Nature, 309*, 431.
Ivanova, L.N., Imshennik, V.S., and Chechetkin, V.M. 1974, *Ap. Space Sci., 31*, 497.
Kawai, Y., Saio, H., and Nomoto, K. 1986, *Ap. J.*, submitted.
Mazurek, T.J., Truran, J.W., and Cameron, A.G.W. 1974, *Ap. Space Sci., 27*, 261.
Miyaji, S., Nomoto, K., Yokoi, K., and Sugimoto, D. 1980, *Pub. Astr. Soc. Japan, 32*, 303
Mochkovitch, R. 1980, Thesis, University of Paris.
———. 1983, *Astr. Ap., 122*, 212.
Nomoto, K. 1980, in *Type I Supernovae*, ed. J. C. Wheeler (Austin: University of Texas), p. 164.
———. 1982a, *Ap. J., 253*, 798.
———. 1982b, *Ap. J., 257*, 780.
———. 1984a, *Ap. J., 277*, 791.
———. 1984b, in *Stellar Nucleosynthesis*, ed. C. Chiosi and A. Renzini (Dordrecht: Reidel), p. 205.
———. 1986a, *Ann. New York Acad. Sci., 470*, 294.
———. 1986b, in *Proceedings of VIth Moriond Astrophysics Meeting: Accretion Processes in Astrophysics*, in press.
Nomoto, K., and Iben, I Jr. 1985, *Ap. J., 297*, 531.
Nomoto, K., Miyaji, S., Yokoi, K., and Sugimoto, D. 1979, in *IAU Colloquium 53, White Dwarfs and Variable Degenerate Stars*, ed. H.M. Van Horn and V. Weidmann (Rochester: Univ. of Rochester), p.56.
Nomoto, K., and Sugimoto, D. 1977, *Pub. Astr. Soc. Japan, 29*, 765.
Nomoto, K., Thielemann, F.-K., and Yokoi, K. 1984, *Ap. J., 286*, 644 (NTY).
Nomoto, K., Thielemann, F.-K., and Wheeler, J.C. 1984, *Ap. J. (Letters), 279*, L23.
Panagia, N., Sramek, R.A., and Weiler, K.W. 1986, *Ap. J. (Letters), 300*, L15.
Saio, H., and Nomoto, K. 1985, *Astr. Ap., 150*, L21.
———. 1986, in preparation.
Sramek, R.A., Panagia, N., and Weiler, K.W. 1984, *Ap. J. (Letters), 285*, L59.
Taam, R.E., and van den Heuvel, E.P.J. 1986, *Ap. J., 305*, 235.
Takahashi, Y., Miyaji, S., Parnell, T.A., Weisskopf, M.C., Hayashi, T. and Nomoto, K. 1986, *Nature, 326*, 839.
Thielemann, F.-K., Nomoto, K., and Yokoi, K. 1986, *Astr. Ap., 158*, 17 (TNY).
Truran, J.W., and Arnett, W.D. 1971, *Ap. Space Sci., 11*, 430.
Unno, W. 1967, *Pub. Astr. Soc. Japan, 19*, 140.
Van den Heuvel, E.P.J. 1984, *J. Ap. Astr., 5*, 209.
Webbink, R. 1984, *Ap. J., 277*, 355.
Webbink, R.F. Rappaport, S., and Savonije, G.J. 1983, *Ap. J., 270*, 678.
Wheeler, J.C., and Harkness, R. 1986, in *Distances to Galaxies and Deviation from the Hubble Flow*, ed. B.M. Madore and R.B. Tully (Dordrecht: Reidel), in press.
Wheeler, J.C., Harkness, R., Barkat, Z., and Swartz, D. 1986, in *Proceedings of the Texas-Mexico Conference on Nebulae and Abundances, Publ. Astr. Soc. Pacific*, in press.
Wheeler, J.C., and Levreault, R. 1985, *Ap. J. (Letters), 294*, L17.
Woosley, S.E. 1986, Saas-Fe Lecture Notes.
Woosley, S.E., Axelrod, R.S., and Weaver, T.A. 1984, in *Stellar Nucleosynthesis*, ed. C. Chiosi and A. Renzini (Dordrecht: Reidel), p.263.
Woosley, S.E., Taam, R.E., and Weaver, T.A. 1986, *Ap. J., 301*, 601.
Woosley. S .E., and Weaver, T.A. 1986a, in *Nucleosynthesis and Its Implications for Nuclear and Particle Physics*, ed. J. Audouze and T. van Thuan (Dordrecht: Reidel).
———. 1986b, *Ann. Rev. Astr. Ap.*, in press.
———. 1986c, in *IAU Colloquium 89, Radiation Transport and Hydrodynamics*, ed. D. Mihalas and K.H. Winkler (D. Reidel: Dordrecht), in press.